Searches for charge-density waves in the alkali metals: Recent neutron-scattering results for sodium

F. J. Lamelas
Department of Physics, Marquette University, Milwaukee, Wisconsin 53233

S. A. Werner
Department of Physics, The University of Missouri, Columbia, Missouri 65211

(Received 3 September 1996)

Neutron-scattering studies of a single crystal of sodium have been carried out at large and small scattering angles. Near the sodium 110 Bragg reflection, we find features which are similar to those which have been observed previously in potassium. Using additional data gathered at small scattering angles, we show that the features near 110 can be quantitatively assigned to an experimental double-scattering artifact, in terms of peak intensities as well as positions. Overall, we find no neutron-scattering evidence of charge-density waves in sodium. [S0163-1829(96)04948-X]

I. INTRODUCTION

The alkali metals are usually thought of as nearly-free-electron (NFE) metals, characterized, for example, by Fermi surfaces which are almost spherical. On the other hand, a series of experimental anomalies in optical, transport, and other measurements has led to an alternative description of the alkali-metal ground state as a charge-density wave (CDW). The fundamental divergence of these contrasting descriptions, combined with necessarily complex interpretations of experimental data, has led to a long-standing debate on the nature of the electronic structure of the alkali metals.[1]

Although many experimental techniques are relevant to this problem, structural measurements are key in the resolution of the controversy. In brief, the CDW model[2] leads to spatial oscillations in the electron density. The oscillations are characterized by an incommensurate wave vector **Q** which spans the Fermi surface. Given any deviation from a perfectly spherical Fermi surface, the wave vectors are oriented along preferred directions and therefore belong to a finite set. In response to oscillations in the electron density, the ion cores are displaced relative to their equilibrium positions with wave vector **Q**, detectable in an x-ray- or neutron-scattering experiment. Although x-ray methods are useful, the greater sample penetration afforded by the neutron-scattering method is advantageous, given that the alkalis form surface impurity layers. Since they are not predicted by other models, an unambiguous observation of Fermi-surface-spanning diffraction satellites in the alkali metals would provide nearly conclusive evidence for a CDW ground state.

A series of scattering experiments has looked for such evidence in potassium. Giebultowicz, Overhauser, and Werner[3] reported an observation of satellites very near the potassium 110 reflection. However, a measurement of weak satellites near a strong reflection is problematic, in that one must carefully separate the satellite intensity from the tail of the strong peak. In fact, in a subsequent neutron-scattering study, Pintschovius *et al.*[4] concluded that the CDW satellites were streaks arising at the potassium 110 peak, due to a double-scattering artifact. At the same time, a synchrotron x-ray experiment by You *et al.*[5] found no evidence for CDW satellites in potassium. In order to study the origin of the instrumental double-scattering effect, Werner *et al.* made a comparative experimental study of silicon and potassium single crystals,[6] followed by a theoretical treatment.[7] Although streaks were found near silicon bulk reflections, their relative weakness suggested that the features observed in potassium were due to more than the double-scattering effect. In another neutron-scattering experiment, Werner, Overhauser, and Giebultowicz[8] reported further evidence of a CDW signature in potassium, found in features near the 220 reflection. However, as pointed out by Pintschovius and Blaschko,[9] the decomposition of the data near 220 into a bulk peak plus two satellites is far from straightforward.

The origin of the double-scattering artifact is shown in Fig. 1. On the left side of the figure, the Ewald-sphere construction of elastic scattering consists of the incident wave vector $\vec{k}_{\rm inc}$, the scattered wave vector $\vec{k}_{\rm sc}$, the scattering vector $\vec{q}$, and the Ewald sphere, indicated by a dashed line. The scattering angle 2θ is the angle between $\vec{k}_{\rm inc}$ and $\vec{k}_{\rm sc}$. For a collimated monochromatic beam incident upon a perfect

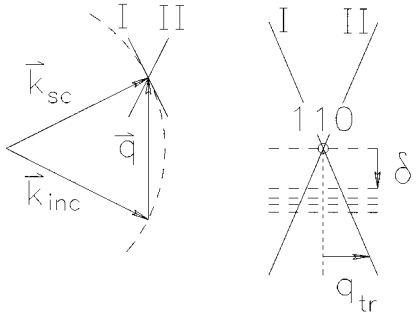

FIG. 1. The left-hand side shows the Ewald-sphere scattering construction and the streaks which may arise due to double scattering within a sample. Streaks I and II are caused by small-angle scattering in the outgoing and incident beams, respectively. The right side of the figure shows the scan trajectories used in gathering the data of Fig. 2.

crystal and using a detector with perfect 2θ resolution, Bragg reflections are measured as points at values of $\vec{q}$ corresponding to the reciprocal lattice of the crystal. On the other hand, suppose that the outgoing beam undergoes small-angle scattering *within the crystal*. In this case, scattering intensities will be measured not just at discrete values of $\vec{q}$, but along a streak in reciprocal space which is tangent to the Ewald sphere, labeled streak I in the figure.[10] A similar consideration of small-angle scattering of the incident beam leads to streak II. The angle between streaks I and II is the scattering angle 2θ. The observation of such streaks in a scattering experiment may be called a double-scattering artifact, but it is not an instrumental resolution effect, since it arises from small-angle scattering within the sample and can in principle be observed even when using a perfect source and perfect 2θ resolution.

In this paper, we report neutron-scattering results for a single crystal of sodium, rather than potassium. The motivation for this work is twofold. First of all, given its fundamental importance, it is worthwhile to test the CDW model in a variety of simple metals. Second, by measuring scattering intensities at both small and large scattering angles, we have performed a quantitative test of the double-scattering effect described above. Apart from its relevance to the scattering issues, our neutron data provide evidence which may be useful in the ongoing analysis of the photoemission results referred to below.

II. EXPERIMENTAL DETAILS

The sodium crystal used in these measurements was grown by the Bridgeman technique. A solid polycrystalline sodium ingot was shaped to fit inside of a stainless-steel tube with a conical tip insert at the lower end. The narrow space between the ingot and the tube was filled with mineral oil until the sodium was fully immersed. Tapered heating coils around the tube allowed the sodium to be melted and then resolidified in a temperature gradient. The crystal was cleaned with xylene and dried in a helium-filled glove bag before being inserted into a thin-walled aluminum sample capsule. The crystal was held by glass wool in the capsule, which was filled with helium gas and sealed by a Teflon gasket. The sample capsule was mounted in a liquid-nitrogen cryostat with aluminum walls, allowing scans to be performed at temperatures ranging from 77 K to room temperature. In contrast to the earlier potassium experiments, we did not perform scans at liquid-helium temperatures, in order to avoid the martensitic transformation to the hexagonal-close-packed structure which occurs in sodium below ~ 36 K.[11] By photographing the Bragg-reflected 110 beam, it was verified that the sample was a single crystal, approximately 35 mm long and 20 mm in diameter. In a rocking curve through the 110 peak, the full width at half maximum (FWHM) was 0.35°.

High-angle data (near sodium Bragg reflections) were taken using the 3XE triple-axis spectrometer at the Missouri University Research Reactor (MURR). The Si (111) monochromator had a mosaic of approximately $18'$; that of the pyrolytic graphite analyzer was $40'$. The collimator settings were $54'/22'/23'/41'$ before and after the monochromator and analyzer. Using a monochromator scattering angle of $2\theta = 44.1°$, the neutron wavelength was 2.35 Å. A 50-mm-thick pyrolytic-graphite filter was used upstream of the sample in order to minimize $\lambda/3$ contamination of the incident beam. Aside from a few surveys, the high-angle data were taken in the $hk0$ scattering plane.

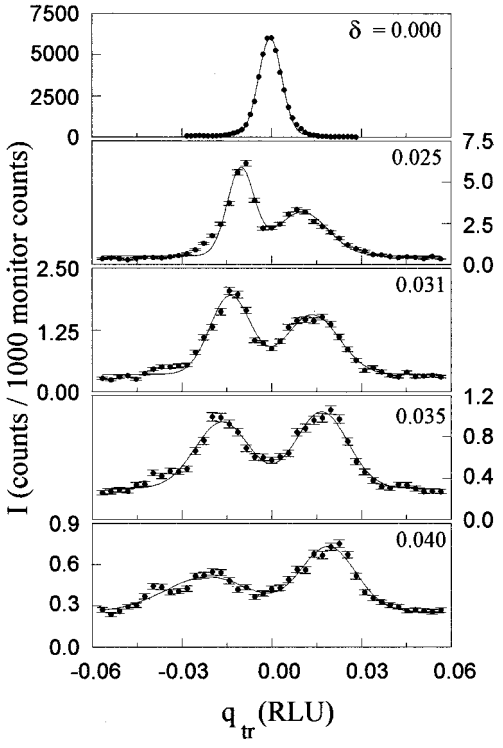

FIG. 2. Elastic neutron-scattering intensities near sodium 110 at $T = 77$ K, along the trajectories indicated in Fig. 1. The data are shown as solid circles, with error bars corresponding to counting statistics. The solid curves are fits to the data using a flat background and two Gaussians. From top to bottom in the figure, the total counting times per data point were 6.8 s, 150 s, 272 s, 408 s, and 680 s.

Small-angle measurements were carried out using the 2XC diffractometer at MURR. With a pyrolytic graphite monochromator set at $\theta = 40.5°$, the wavelength was 4.35 Å. No analyzer was used in this setup; the collimator settings were $54'/17'/20'$ before and after the monochromator, and between the sample and detector. A liquid-nitrogen-cooled polycrystalline beryllium filter was used between the monochromator and the collimator defining $\vec{k}_{\rm inc}$.

III. RESULTS

Initial high-angle scans were performed near the sodium 110 peak, in order to check for those features which have previously been observed in potassium.[3] These data, shown in Fig. 2, were all taken at $T = 77$ K. The right-hand side of Fig. 1 shows the trajectories of these scans as dashed lines, along with streaks I and II, drawn with a relative orientation 2θ equal to the 46.4°, the scattering angle for sodium 110 at $T = 77$ K. In Figs. 2 and 3, scattering vectors are labeled according to their transverse components $q_{\rm tr}$ and their longitudinal components δ, relative to the sodium 110 peak. Scattering vectors are plotted in reciprocal lattice units (RLU),

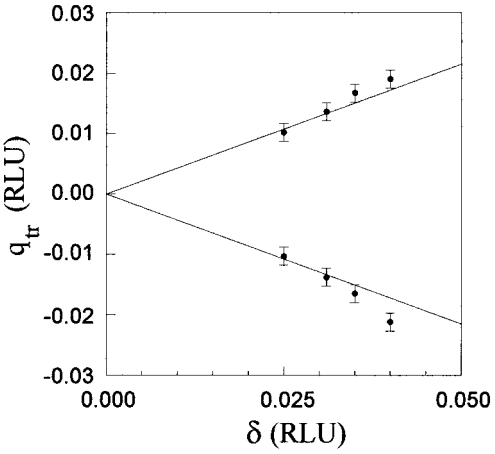

FIG. 3. Positions of the peaks in Fig. 2. Transverse peak positions are plotted as a function of the longitudinal displacement δ which characterizes each scan. The solid lines are calculated assuming that two streaks separated by 46.4° originate at the sodium 110 Bragg reflection.

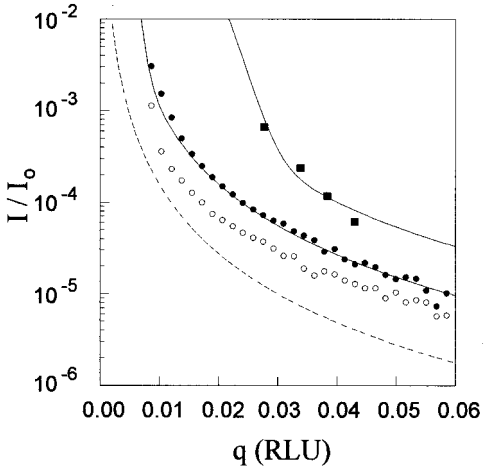

FIG. 4. Comparison of high-angle data (squares) and low-angle data (points) with an *ad hoc* intrinsic small-angle scattering function (dashed curve) after folding with Gaussians of width 0.005 RLU (lower solid curve) and 0.01665 RLU (upper solid curve). The solid squares are normalized peak intensities in scans through streaks near 110; the solid and open circles are small-angle scattering intensities with and without an enclosing cryostat.

where 1 RLU $= 2\pi/a$ and a is the lattice parameter of sodium. In order to eliminate any artifacts arising in $\lambda/3$ neutrons, the peaks in Fig. 2 were also scanned without the graphite filter; the resulting intensity verified that these features are due to 2.35 Å neutrons, not $\lambda/3$.

Qualitatively, the sodium features are similar to those of potassium. In analyzing the data of Fig. 2, the main question to be answered is whether the two peaks shown in the lower four panels correspond to discrete satellites of the sodium 110 peak or streaks emerging from the 110 peak. To address this question, there are two specific signatures which distinguish satellites from the streaks which would arise from the double-scattering artifact. First, if the peaks shown in Fig. 2 are cross sections of streaks, their *positions* will define two lines which pass through 110 with a relative angle of $2\theta = 46.4°$. Second, an origin in double scattering would give rise to *intensities* which fall off monotonically with a dependence characteristic of the small-angle scattering in the sample-cryostat system.

The issue of peak positions is addressed in Fig. 3. We have taken the fitted transverse peak positions from the lower four panels of Fig. 2 and plotted them as a function of δ, the longitudinal displacement of each scan relative to the sodium 110 peak. The error bars on the peak positions were estimated by inspection of Fig. 2. The solid lines in Fig. 3 are peak positions calculated assuming two streaks rotated by 46.4°. It is clear that the peak positions are consistent with an origin in the double-scattering effect.

In order to compare the peak intensities of Fig. 2 with those due to double scattering, consider streak I of Fig. 1. Since the intensity along streak I arises from small-angle scattering of the outgoing (Bragg-diffracted 110) beam, its form as a function of q along the streak will be identical to that of the small-angle scattering intensity. (By q we mean the scattering vector relative to 110.) In order to compare intensities, the streak intensities are normalized with respect to the 110 peak intensity, and the small-angle data are normalized to the incident beam intensity.[12]

The solid squares in Fig. 4 are the normalized peak intensities from the lower four panels of Fig. 2. In order to plot these as a function of q along the streaks, we take $q = \delta/\cos(\theta_{110}) = \delta/\cos(23.2°)$, where δ is the longitudinal displacement (Fig. 1) and 23.2° is the 110 Bragg angle for $\lambda = 2.35$ Å neutrons. The circles in Fig. 4 are the small-angle scattering data, where the solid circles were measured with the sample in the cryostat and the open circles with the sample in its capsule but out of the cryostat. Since an earlier set of data taken under identical conditions showed that the small-angle-scattering intensities are essentially identical at $T = 77$ K and at room temperature, the small-angle data of Fig. 4 were taken at room temperature, in order to compare intensities with the sodium sample capsule in and out of the cryostat. The scattering vector is given in RLU by $q = (4\pi\sin\theta/\lambda)(a/2\pi) = 2a\sin\theta/\lambda$. Using a conventional approach, the small-angle data were background corrected as follows:

$$I = \frac{1}{T}[I(q) - I(bkg)] - [I_0(q) - I_0(bkg)],$$

where $I(q)$ and $I_0(q)$ are the measured intensities with a sample in place and no sample in place. $I(bkg)$ and $I_0(bkg)$ are the asymptotic (high-angle) intensities with and without a sample in place, and T is the transmission of the sample, equal to 0.77 with the cryostat in place and 0.79 without it (for $\lambda = 4.35$ Å neutrons). After background correction, the small-angle data were normalized to the incident beam intensity for comparison with the data near 110.

Before describing the solid and dashed curves of Fig. 4, it is useful to compare the three sets of data qualitatively. First, note that the small-angle intensities with and without the cryostat are similar in form and differ in magnitude by a factor of approximately 2. It is difficult to assign this ratio with great precision, since the sodium crystal was approximately cylindrical, tilted by an angle of roughly 30°, leading to variations in the small-angle scattering intensity as a func-

tion of the orientation of the scattering vector. However, by comparing data from several runs, we conclude that for this particular sample and cryostat, at least half of the small-angle scattering intensity originates within the sample and its aluminum capsule. The second qualitative feature of Fig. 4 concerns relative intensities at small angles and near 110: The high-angle intensities are a factor of 3–10 higher than the small-angle intensities.

This apparent discrepancy can be resolved by a more careful look at the double-scattering effect. Our discussion so far has assumed a perfectly collimated source and perfect detector resolution, in short, perfect instrumental resolution. In practice, the effect of instrumental resolution in these measurents is dramatic: Intensities in the tail of a rapidly varying function will vary strongly if the central peak width is changed. Referring to Fig. 1, the relevant resolution in small-angle scattering is the longitudinal resolution, which we have determined by scanning the detector through the incident beam. This ''arm zero'' peak can be fitted as a Gaussian with a full width at half maximum (FWHM) of 0.007 RLU. At high angles (near 110), the streak intensities will be affected by a combination of the instrumental width and the intrinsic width of the 110 Bragg reflection, in the direction parallel to the streak. As a reasonable approximation, we use the width obtained by fitting a longitudinal scan through 110 (a direction 23.2° from the streak direction) with a Gaussian; its FWHM is 0.015 RLU. In other words, the intensities near 110 are not obviously inconsistent with double-scattering streaks, once we take the relevant experimental widths into consideration.

To complete this argument, the solid curves in Fig. 4 were generated by adopting an *ad hoc* form of the intrinsic small-angle scattering intensity and folding it with Gaussians of two separate widths. In trying a reasonable form of the small-angle scattering intensity, we began by noting that our small-angle data are essentially linear on a log-log plot, corresponding to a function of the form $I=cq^{-2.5}$, where c is a constant.[13] This function diverges at $q=0$; thus in order to plot normalized intensities of the form $I(q)/I(0)$ (shown by the dashed curve) a flat upper bound of the function was put in by hand at $q=0.0003$ RLU. The lower solid curve, which passes through the low-angle data, was generated by folding the dashed curve with a Gaussian of width 0.005 RLU. The upper solid curve (through the data near 110) was produced with a Gaussian width of 0.016 65 RLU. Given the approximations used in this procedure, these values agree quite well with the corresponding measured widths of 0.007 RLU and 0.015 RLU. That is, once the appropriate resolution functions are taken into account, the data of Fig. 2 are consistent with double-scattering streaks, in terms of *intensities* as well as positions.

An inherent difficulty in neutron scattering with a triple-axis spectrometer is the combination of point-by-point detection (which allows one to access a single-scattering vector at a time) and a relatively low beam flux: It is difficult to survey broad areas of reciprocal space within reasonable periods of time. Within these constraints, and since the features near 110 (Fig. 2) may not be assigned as CDW satellites, we performed several broad searches in the neighborhood of the sodium 220 Bragg reflection. In Fig. 5, the square near 220 indicates the corresponding area covered by the scans of Fig. 2. The broader surveys were carried out along the trajectories given by the dashed lines. In order to look for satellites out of the $hk0$ plane, these scans were repeated after tilting the sample by 2° about a horizontal axis. No unusual features attributable to CDW satellites were found in any of the broad surveys.

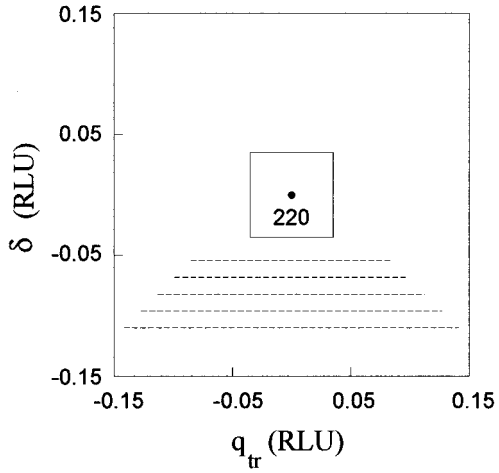

FIG. 5. Diagram of the region of the $hk0$ plane in which CDW searches were performed for this study. The data of Fig. 2 were taken in a region corresponding to that enclosed by the solid square; additional survey scans were performed along the trajectories given by the dashed lines.

IV. DISCUSSION

There are a number of features of the earlier neutron data for potassium which were interpreted as providing evidence for the CDW picture; these should be reevaluated in light of our present study. First, a weaker streak intensity was observed in silicon crystals, even when mounted in a cryostat[9] or in an aluminum tube simulating a cryostat.[6] Since we have found that half or more of the small-angle scattering occurs within the sample and its capsule, it is clear that the double-scattering streaks need not be due to the walls of the cryostat; they can arise due to small-angle scattering in the alkali metal crystal, the surrounding glass wool, or the walls of the aluminum capsule. In other words, to analyze the streak intensity of a given sample, the appropriate comparison is with the small-angle scattering in that sample, not the streak intensity in a completely different sample such as silicon.

A second question has involved scattering near 220, where the double-scattering streaks have been difficult to observe.[8] In retrospect, this difficulty is not surprising. First of all, the streak intensities are relatively weak even near 110, and they fall off very quickly as a function of q along the streak (Fig. 4, solid squares). In addition, since the angle between the streaks increases with scattering angle, near 220 the distance along the streak is significantly greater than at 110, given a specific longitudinal shift δ from the Bragg point (Fig. 1). The ratio of these distances is given by $\cos(\theta_{110})/\cos(\theta_{220})=1.49$, where θ_{110} and θ_{220} are the Bragg angles at 110 and 220. Given a $q^{-2.5}$ form of the streak intensity, this effect leads to a drop in the relative streak intensity by a factor of ~ 2.7 at 220 vs 110. Since the

220 Bragg intensity is weaker than at 110 by a factor of ~ 2.5,[8] one expects the absolute streak intensities at 220 to be $\sim 15\%$ of those at 110, at a given longitudinal shift δ. In addition to this effect (but depending on the monochromator angle) the instrumental resolution near 220 can be significantly worse than at 110, requiring much tighter collimation in order to approach the Bragg reflection closely. All of these effects make it difficult to observe the double-scattering streaks near 220 in sodium and potassium. In retrospect, it is now clear that double-scattering streaks near 220 could not have been detected under the experimental conditions corresponding to Fig. 4(b) of Ref. 8, since their intensities would have been buried in the background.

It is interesting that apart from the structural (neutron- and x-ray-scattering) measurements, a series of conflicting experimental and theoretical papers has treated photoemission in the alkali metals. Although in principle photoemission should offer a means of direct comparison of NFE and CDW models of electronic structure, the theoretical interpretation of the experiments remains unresolved. Following quickly after Overhauser's initial interpretation[15] of photoemission data for sodium[14] according to a CDW model, Shung and Mahan[16] reported that these data can also be explained using a NFE band. This did not settle the issue: In a succeeding experimental study, Itchkawitz, Lyo, and Plummer[17] found a qualitative difference in the Fermi-level structure of potassium, relative to that of sodium. This result indicated that a readjustment of the NFE model could be necessary in order to explain both the sodium and potassium data simultaneously. On a somewhat different track, after low-energy-electron-diffraction measurements of potassium, Itchkawitz *et al.*[18] avoided the NFE vs CDW issue altogether and suggested the formation of martensitic embryos as a possible explanation for their observation of a surface shear structure. Recently, and most relevant to the neutron-scattering controversy, Ma and Shung[19] reported that the inclusion of a CDW is necessary in order for their calculations to reproduce the photoemission data[17] for potassium, a result which contrasts sharply with the earlier sodium calculation.[16]

The neutron-scattering data are an important component in the ongoing effort to characterize the alkali metals by techniques such as photoemission or transport.[1] Based on our data for sodium and in light of our examination of the existing potassium data,[3–9] we conclude that no clear-cut evidence for the existence of charge-density waves in the alkali metals is to be found in the scattering experiments which have been performed to date. The neutron data do not disprove the CDW model of the alkali metals, but we now feel that they cannot be cited as evidence for it. We also note that the current data should not preclude future CDW searches in the alkalis, since it is entirely possible that more sensitive neutron- and x-ray-scattering techniques may succeed where previous attempts have failed.

Our experiment may be summarized as an extension of the CDW search to sodium, an archetypical simple metal. We find no evidence for charge-density waves in the sodium diffuse-scattering data. Going beyond previous neutron-scattering measurements, we have shown that by measuring small-angle scattering intensities the streaks near sodium 110 can be assigned to double scattering, in terms of intensities as well as positions. In the light of the analysis presented above, we essentially agree with the double-scattering interpretation of the potassium data initially proposed by Pintschovius *et al.*[4] We hope that our work will clarify the existing neutron data for the alkali metals from a scattering viewpoint, as well in its relevance to current efforts in experiment and theory.

ACKNOWLEDGMENTS

This work was made possible by NSF Grant No. PHY-9024608. F.J.L. is grateful to MURR for partial salary support during the period when these measurements were made. A. W. Overhauser made practical contributions and gave important advice throughout this experiment. K. W. Herwig provided essential assistance in measurements at 2XC.

[1] Jack Bass, William P. Pratt, Jr., and Peter A. Schroeder, Rev. Mod. Phys. **62**, 645 (1990).

[2] A. W. Overhauser, in *Highlights of Condensed-Matter Theory*, Proceedings of the International School of Physics ''Enrico Fermi,'' edited by F. Bassani, F. Fumi, and M. P. Tosi (North-Holland, Amsterdam, 1985), p. 194.

[3] T. M. Giebultowicz, A. W. Overhauser, and S. A. Werner, Phys. Rev. Lett. **56**, 1485 (1986).

[4] L. Pintschovius, O. Blaschko, G. Krexner, M. de Podesta, and R. Currat, Phys. Rev. B **35**, 9330 (1987).

[5] Hoydoo You, J. D. Axe, Dietmar Hohlwein, and J. B. Hastings, Phys. Rev. B **35**, 9333 (1987).

[6] S. A. Werner, T. M. Giebultowicz, and A. W. Overhauser, Phys. Scr. **T19**, 266 (1987).

[7] S. A. Werner and M. Arif, Acta Crystallogr. A **44**, 383 (1988).

[8] S. A. Werner, A. W. Overhauser, and T. M. Giebultowicz, Phys. Rev. B **41**, 12 536 (1990).

[9] L. Pintschovius and O. Blaschko, Phys. Rev. B **44**, 10 361 (1991).

[10] Note that streak I is reminiscent of the instrumental resolution function corresponding to a collimated incident beam and comparatively poor 2θ resolution; however, its origin is completely different.

[11] See, for example, W. B. Pearson, *A Handbook of Lattice Spacings and Structures of Metals and Alloys* (Pergamon, New York, 1958).

[12] In comparing relative intensities near the origin and near 110 it is not necessary to include an extinction correction: The 110 intensity and the streak intensities share the same factor, which cancels after normalization.

[13] Our aim here is not to model the small-angle scattering intensity; thus the form of this function is solely to be regarded as a fitting parameter used in comparing the small-angle and high-angle data.

[14] E. Jensen and E. W. Plummer, Phys. Rev. Lett. **55**, 1912 (1985).

[15] A. W. Overhauser, Phys. Rev. Lett. **55**, 1916 (1985).

[16] Kenneth W.-K. Shung and G. D. Mahan, Phys. Rev. Lett. **57**, 1076 (1986).
[17] B. S. Itchkawitz, In-Whan Lyo, and E. W. Plummer, Phys. Rev. B **41**, 8075 (1990).
[18] B. S. Itchkawitz, A. P. Baddorf, H. L. Davis, and E. W. Plummer, Phys. Rev. Lett. **68**, 2488 (1992).
[19] Shih-Kuei Ma and Kenneth W.-K. Shung, Phys. Rev. B **50**, 5004 (1994).